PNNL- 14277

Pacific Northwest
National Laboratory
Operated by Battelle for the
U.S. Department of Energy

Possible Incorporation of Neptunium in Uranyl (VI) Alteration Phases

E. C. Buck
B. K. McNamara
M. Douglas
B. D. Hanson

November 2003

Prepared for the U.S. Department of Energy
under Contract DE-AC06-76RL01830

DISCLAIMER

PACIFIC NORTHWEST NATIONAL LABORATORY
operated by
BATTELLE
for the
UNITED STATES DEPARTMENT OF ENERGY
under Contract DE-AC06-76RL01830

PNNL-14277

Possible Incorporation of Neptunium in Uranyl (VI) Alteration Phases

E. C. Buck
B. K. McNamara
M. Douglas
B. D. Hanson

November 2003

Prepared for the U.S. Department of Energy
under Contract DE-AC06-76RL01830

Pacific Northwest National Laboratory
Richland, Washington, 99352

Summary

This report examines the ability of Electron Energy-Loss Spectroscopy (EELS) on the Transmission Electron Microscope (TEM) to detect low levels of neptunium (Np) in a uranium matrix and in the possible presence of rare earth and transuranic elements. Verification of this technique is necessary to support the case for using uranium (VI) secondary minerals from corroded spent fuel as the solubility-controlling phases for Np in the Yucca Mountain performance assessment model. In this report, the use of EELS to detect Np at low levels in uranium phases is examined through analysis of data from spent fuel tests and synthesis tests. Because TEM-EELS is a high spatial resolution technique it provides one of the most suitable methods for probing the nature of sub-micron multiphase solids, such as those formed during the corrosion of spent fuel.

The detection of Np in a matrix of uranium (U) can be impeded by the occurrence of a plural scattering event from U ($U\text{-}M_5 + U\text{-}O_{4,5}$) that results in severe overlap on the $Np\text{-}M_5$ edge at 3665 eV. By examining the energy gap between the $Np\text{-}M_5$ and $Np\text{-}M_4$ edges (184 eV), a method for observing Np independently of the plural scattering event has been established, confirming earlier results suggesting co-precipitation of Np and U in some solids. Clear evidence of Np incorporation into studtite and uranophane has been found in laboratory tests using EELS. Preliminary results from the examination of a spent fuel solid with radiochemical methods suggests limited uptake of Np into the uranyl (VI) alteration phase.

The objective of this work was to evaluate the application of EELS on the Transmission Electron Microscope (TEM) for detecting Np in a U matrix. A series of limited tests were run to determine possible evidence of Np incorporation into uranyl (VI) solids. EELS data on Np solids at ANL were re-examined. Synthesized Np-doped uranyl phases were examined with X-ray diffraction (XRD), Raman, Optical Microscopy, and TEM-EELS. Microstructural and radiochemical analysis of alteration phases from a series of preliminary spent fuel tests was performed. A new method for providing improved data on Np concentrations with EELS was tested on a series of mineral phases.

The development of a set of standards for the Yucca Mountain Program to improve future Np analyses with analytical techniques would be beneficial.

References

EC Buck, RJ Finch, PA Finn, and JK Bates. 1998. "Retention of neptunium in uranyl alteration phases formed during spent fuel corrosion." *Mater. Res. Soc. Symp. Proc.* 506:87-94.

Acronyms

ANL	Argonne National Laboratory
ATM	Approved Testing Material
CSNF	Commercial Spent Nuclear Fuel
EDS	Energy Dispersive X-Ray Spectroscopy
EELS	Electron Energy-Loss Spectroscopy
EMSL	Environmental Molecular Sciences Laboratory
IR	Infrared Spectroscopy
KPA	Kinetic Phosphorescence Analysis
ICM-MS	Inductively Coupled Plasma-Mass Spectrometry
IR	Infrared
ORIGEN2	Isotope Generation and Depletion Code
PEELS	Parallel EELS
PNNL	Pacific Northwest National Laboratory
SEM	Scanning Electron Microscopy
TEM	Transmission Electron Microscope
TRU	Transuranic
XAS	X-Ray Absorption Spectroscopy
XRD	X-Ray Diffraction

Definitions

Absorption Edge	Is generated at an energy where the scattering probability jumps due to an ionizing transition.
Alteration Phase	A phase formed following corrosion of the primary phase.
$M_{4,5}$-Edges	Resulting from transitions from 3*d* level to unoccupied 5*f* levels and continuum states.
Plural Scattering	In EELS, occurs when an electron passing through sample undergoes multiple scattering events. The resultant energy-loss signal is the sum of inelastic losses.
Spectrum	In this report, refers to a plot of measured intensity versus electron or x-ray energy.

Mineral Names and Formulae used in the Report

MINERAL NAME	FORMULA
Boltwoodite	$K_2(UO_2)_2(SiO_3)_2(OH)_2 \cdot 5H_2O$
Compreignacite	$K_2O \cdot 6UO_2 \cdot 11H_2O$
Dehydrated Schoepite	$UO_3 \cdot 0.8H_2O$
Meta-Schoepite	$[(UO_2)_8O_2(OH)_{12}](H_2O)_6$
Meta-Studtite	$[UO_2(O_2)(H_2O)_2](H_2O)$
Soddyite	$(UO_2)_5(SiO_4)_2(OH)_2 \cdot 5H_2O$
Studtite	$[UO_2(O_2)(H_2O)_2](H_2O)_2$
Uraninite	UO_2
Uranophane	$Ca(UO_2)_2(SiO_3)_2(OH)_2 \cdot 5H_2O$
Weeksite	$K_2(UO_2)_2(Si_2O_5)_3 \cdot 4H_2O$

Unit Abbreviations

at%	Atomic percent
°C	degrees Centigrade
cm^{-1}	wavenumber
eV	electron volt
g	gram
keV	kilo-electron volt
µg	microgram
µm	micrometer
M	molarity / mole
mg	milligram
mL	milliliter
nm	nanometer
wt%	weight percent

Acknowledgements

The transmission electron microscopy work was performed at the Environmental Molecular Sciences Laboratory, a national scientific user facility sponsored by DOE's Office of Biological and Environmental Research and located at Pacific Northwest National Laboratory, operated for DOE by Battelle under Contract DE-AC06-76RL01830.

Contents

Figures

Tables

1.0 Introduction

Many countries, including those with active fuel-reprocessing facilities, are planning to dispose of commercial spent nuclear fuel (CSNF) from nuclear reactors. The CSNF may be either sent to a permanent geologic repository or to an interim storage facility. It is unlikely that all water can be completely removed from the CSNF casks; in addition, over time, some casks are expected to fail, allowing small amounts of water to contact the fuel. Due to its high radiation field, CSNF in contact with water may undergo oxidative dissolution under both oxidizing and reducing environments by the formation of reactive radiolysis products. Dissolution of natural uraninite (UO_2) (Finch and Ewing 1992) and synthetic UO_2 (Wronkiewicz et al. 1992) can result in the formation of a series of U(VI) secondary phases, such as uranyl oxide hydrates (e.g., meta-schoepite), uranyl silicates (e.g., uranophane), phosphates, or carbonates, depending on the composition of the contacting water. However, in CSNF, less is known about the fate of the fission and neutron capture products that may result in the precipitation of unique alteration phases, depending on the availability of these species in the fuel matrix. Burns et al. (1997) have theorized that many of the U(VI) alteration phases may be capable of incorporating several key radionuclides, including neptunium (Np), technetium (Tc), and plutonium (Pu). Cesium (Cs), barium (Ba), and molybdenum (Mo) have been observed to be incorporated into a unique U(VI) phase related to billietite (Buck et al. 1997).

This study examines existing data on Np behavior from both spent fuel and glass tests in an effort to resolve some issues concerning the selection of possible solubility limiting phases for Np and the methods for detecting Np at low levels in spent fuel. This report examines the ability of Electron Energy-Loss Spectroscopy (EELS) on the Transmission Electron Microscope (TEM) to detect low levels of neptunium (Np) in a uranium matrix and in the possible presence of rare earth and transuranic elements. Verification of this technique is necessary to support the case for using uranium (VI) secondary minerals from corroded spent fuel as the solubility-controlling phases for Np in the Yucca Mountain performance assessment model. In this report, the application of EELS to detect Np at low levels in uranium phases is examined through analysis of data from spent fuel tests and synthesis tests. Because TEM-EELS is a high spatial resolution technique it provides one of the most suitable methods for probing the nature of sub-micron multiphase solids, such as those formed during the corrosion of spent fuel.

A major problem with the analysis of CSNF with any elemental-analysis method is that the level of many key elements is at or below detection limits. Techniques that typically have sufficient limits of detection may not have the required spatial resolution to examine the nano-sized corrosion products of CSNF. It is possible to establish the association of Np or other elements with a particular U phase, but only a microscopy technique with high spatial resolution can be used to determine whether the element is incorporated into the phase of interest.

The work with CSNF and borosilicate glass with EELS has allowed the detection of rare-earth elements and the major actinide (Pu) (Buck and Fortner 1997; Buck 1999). The detection of Np is important to establish that its long-term behavior is necessary for developing models.

2.0 Experimental Procedure

The CSNF used in this study was Approved Testing Material (ATM)-106, ATM-103, and ATM-101 with average burn-ups of 45, 33, and 31 MWd/kgU, respectively (Guenther et al. 1986). Tests run at Argonne National Laboratory (ANL) used spent-fuel fragments placed on a Zircaloy retainer inside a steel test vessel exposed to moderate amounts of water (Finn et al. 1994). The atmosphere in the reaction vessel was limited in oxygen; however, the radiation field generated by the fuel itself produced an oxidizing environment. In tests at Pacific Northwest National Laboratory (PNNL), ATM-101 was reacted with deionized water for periods up to two years. In addition, laboratory synthesis of neptunium-doped U(VI) phases was carried out at PNNL (Douglas et al. 2003). These phases were examined with electron microscopy, x-ray diffraction, and infrared spectroscopy. The results of EELS examinations are reported here.

During a limited number of sampling periods during the drip tests at ANL, random samples of corroded spent fuel were extracted from the test vessel and examined with optical and scanning electron microscopy. Given the nature of the sample preparation process and the difficulty of extracting samples in a hot cell, it is not possible to know whether these selected particles were representative of the entire sample. Micron-sized particles from these extracted particles were then embedded in an epoxy resin and thin-sectioned with an ultramicrotome. The electron-transparent thin-sections of the corroded spent fuel were laid on 200-mesh carbon-coated copper grids and examined with a 200-keV transmission electron microscope with an attached Gatan Image Filter (GIF) for electron energy-loss spectroscopy and an x-ray energy dispersive spectrometer. The EELS energy resolution was 1.5 to 2.0 eV at the M-edges of the rare earth elements (REE) and 4 to 5 eV at the M-edges of the transuranics (TRUs).

The initial investigations were performed with a Gatan parallel EELS (PEELS) system and later with the much more efficient Gatan Image Filter (GIF200) attached to a JEOL2000FXII Transmission Electron Microscope (TEM) at ANL and the JEOL2010 TEM with attached GIF2000 image filter at the Environmental Molecular Sciences Laboratory (EMSL) at PNNL. Two techniques were used to confirm the presence of elements in the fuel samples, the peak position based on values reported in the literature, and the peak-to-peak separation. Analyses were performed with second difference imaging, using a unique script within the Gatan, Inc. software for this purpose (Buck 1999). Second-difference spectroscopy requires three spectra to be collected in series offset by a set energy difference, typically equal to the peak width (4 to 6 eV). Electron energy-loss spectroscopy can detect rare-earth elements at ppm levels in spent fuel (Buck 1999). The absorption edges are often displaced 3 to 5 eV from the nominal positions reported in the literature, possibly due to changes in the chemistry of the analyzed elements (See Table 2.1).

During two sampling periods (44 and 48 months), random samples of corroded spent fuel were extracted from the Argonne CSNF unsaturated test vessels and examined. Given the nature of the sample-preparation process and the difficulty of extracting samples, it was not possible to know whether these selected particles were representative of the entire sample. Micron-sized particles from these extracted particles were then embedded in an epoxy resin and thin-sectioned with an ultramicrotome. The electron-transparent thin-sections of the corroded spent fuel were laid on 200 mesh carbon-coated copper grids and examined.

Of particular interest in the actinide series is the detection of Np. Np is characterized by two sharp M-edges at 3665 eV (M_5) and 3850 eV (M_4); however, the Np-M_5 "white-line" is nearly coincident with a plural scattering peak from U (see Table 2.1). This additional peak is the result of a U-$O_{4,5}$ (~95 to 113 eV) event combined with the U-M_5 edge at 3552 eV, resulting in a broad (~12 to 18 eV) peak near 3665 eV. However, the Np-M_4 peak is not subject to similar interference and is separated from the plural event

on the U-M_4 edge by 7 to 8 eV. Hence, the method adopted in this study has been to look for evidence of the Np-M_4 peak and its separation from the more intense peak typically observed near 3665 eV. All spectra were calibrated internally from the assumed 176-eV energy separation of the U M_5 and M_4 edges. The separation of the M_4 and M_5 edges for U, Pu, and Np was checked using a standard sample with large concentrations of these particular elements (see Figure 2.1). The energy separation agrees with literature values.

The plural effect was clearly visible in many collected U spectra; however, its effect was reduced by using very thin samples, optimizing the energy resolution, and reducing counting times. Reducing the energy dispersion will also allow more accurate separation of features near both Np-M edges by increasing the number of channels between the features. However, if the energy width of the U-M 'white-lines' is larger than 8 eV, it may be impossible to distinguish plural events from absorption edges.

Table 2.1. Absorption Edge Energies[(a)] for Actinide Elements (values in eV)

	N_5	N_4	ΔE ($N_{4,5}$)	M_5	M_4	ΔE ($M_{4,5}$)
Th	676	714	38	3332	3491	159
U	738	780	42	3552	3728	176
Np	**770**	**816**	**46**	**3666**	**3850**	**184**
Pu	801	850	49	3778	3973	196
Am	828	879	51	3887	4092	205

(a) Data taken from the Handbook for Chemistry and Physics, 63rd. Edition, 1982-1983, CRC Press.

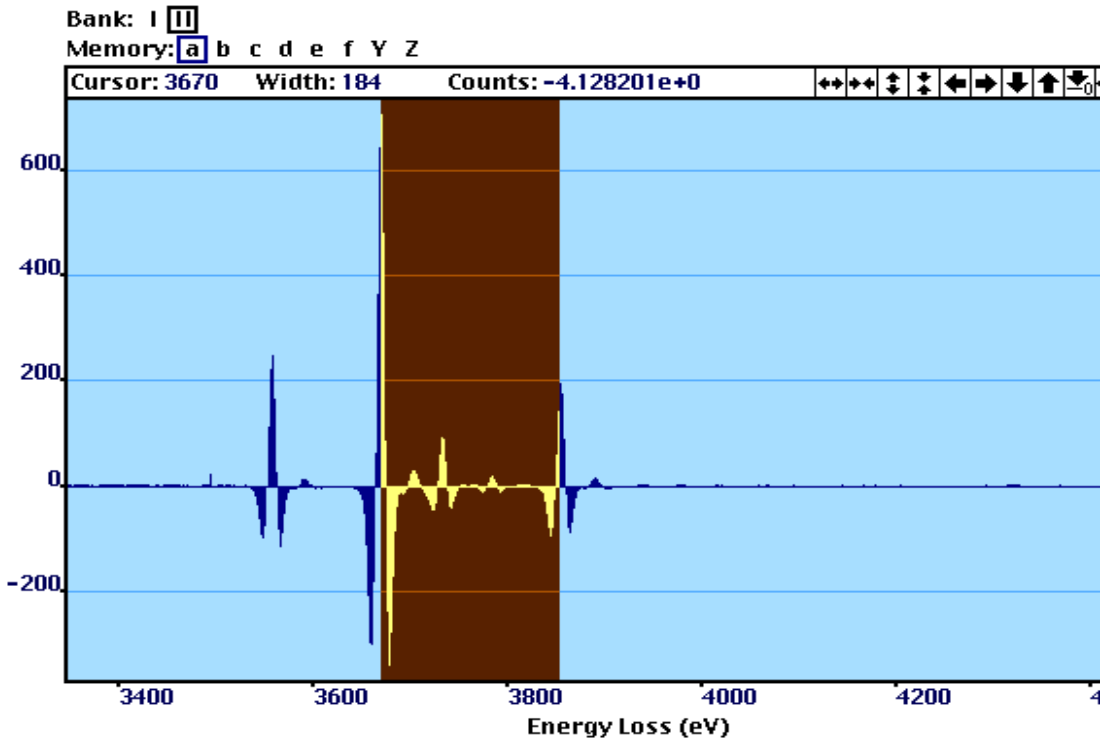

Figure 2.1. Standard Sample Containing U, Np, and Pu. The window shows the energy separation between the Np-M_5 and Np-M_4 edges of 184 eV. The spectrum has been collected in second difference mode on a Gatan Image Filter.

3.0 Np in Spent Fuel

As the plural scattering peak from U overlaps in the region where we expect to observe the Np-M_5 edge, we have used the expected separation in energy between the two intense M-edges from Np. Figure 3.1 through Figure 3.3 shows the separation of two weak features from a sample of CSNF. An energy window 184 eV wide demonstrates the separation. A plural peak on the U M_4 edge would be separated from the Np-M_4 peak by 8 eV. Indeed, this peak is observed in Np-free spectra and is separated from the lower energy plural peak by 176 eV. If the energy resolution obtained is sufficient, it should be possible to distinguish plural events from the actual presence of Np using the higher energy M-edge.

Another piece of evidence comes from comparing the intensity ratios of the two features in the Np spectrum. This is reported as the M_4/M_5 intensity ratio. If the features are entirely due to plural scattering, then the intensity ratio of the plural peak should be the same as the intensity ratio of the U-M_4/M_5 peaks (0.45). For the pure standard Np sample (see Figure 2.1), the M_4/M_5 ratio is close to 0.28. From three analyses of Np features in actinide EELS spectra, ratios of 0.3, 0.28, and 0.3 were observed.

The intensity ratio of the U-M_4/M_5 is 0.46 and is equal to the intensity ratio of the plural peaks. The separation between the two plural peaks is 176 eV. The effect of superimposing a pure U-M spectrum on itself and shifting by 176 eV results in a perfect overlap at the plural peak position. The fact that a similar operation on the spectrum shown in Figure 3.1 through Figure 3.3 results in a resolvable separation of near 8 eV is proof that Np can be detected with EELS at low levels. In Figure 3.4, an Np spectrum has been overlaid on a U-only spectrum. The plural peaks are visible as broad humps. The Np-M_4 edge does not match with the plural hump from the U.

3.1 Alteration Phase Analysis

A major issue is whether there is any evidence of Np incorporation into alteration phases in the CSNF tests. In Figure 3.5, EELS analysis of an alteration phase from the ANL drip tests is shown. Further evidence is shown in the spectra in Figure 3.6. In this case, a 176-eV window does not match the two features on the spectrum; however, a window of 184 eV does resolve this issue.

The window between the two features is near the assumed positions for Np-M_5 and Np-M_4. If the features were entirely due to plural scattering, the peak-to-peak separation would not be near 184 eV. This is proof that, at least in this case, Np is most likely present in the phase. Spectrum has been superimposed on itself and shifted by 176 eV. The separation is near 6 eV, not the ideal value of 7.5 eV, but this is further evidence that the peaks are not solely due to plural scattering and that the phase likely contains Np.

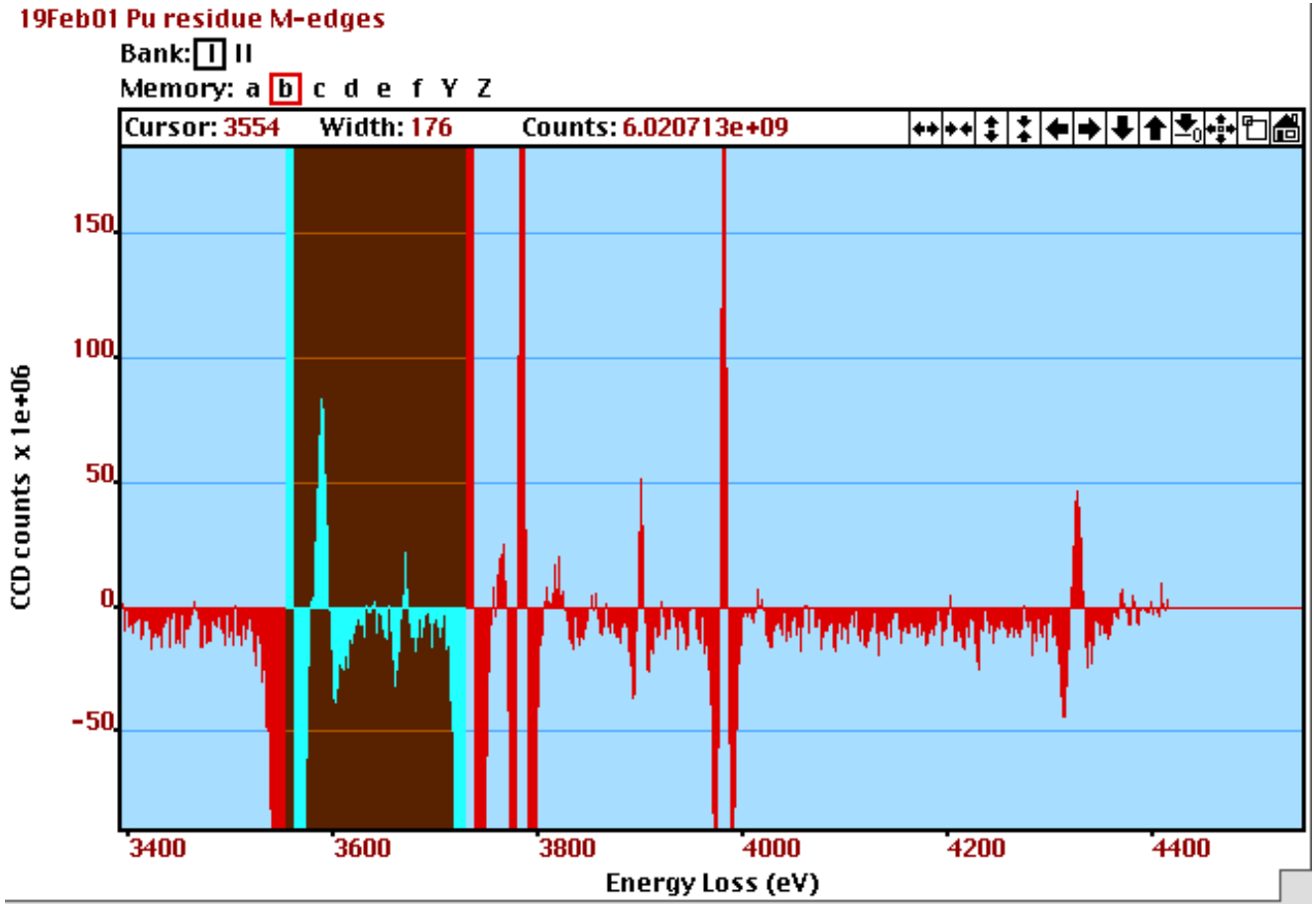

Figure 3.1. EELS of CSNF Material Showing Separation of 184 eV Between the Two Features Corresponding to the Np-M_5 and Np-M_4 Peaks

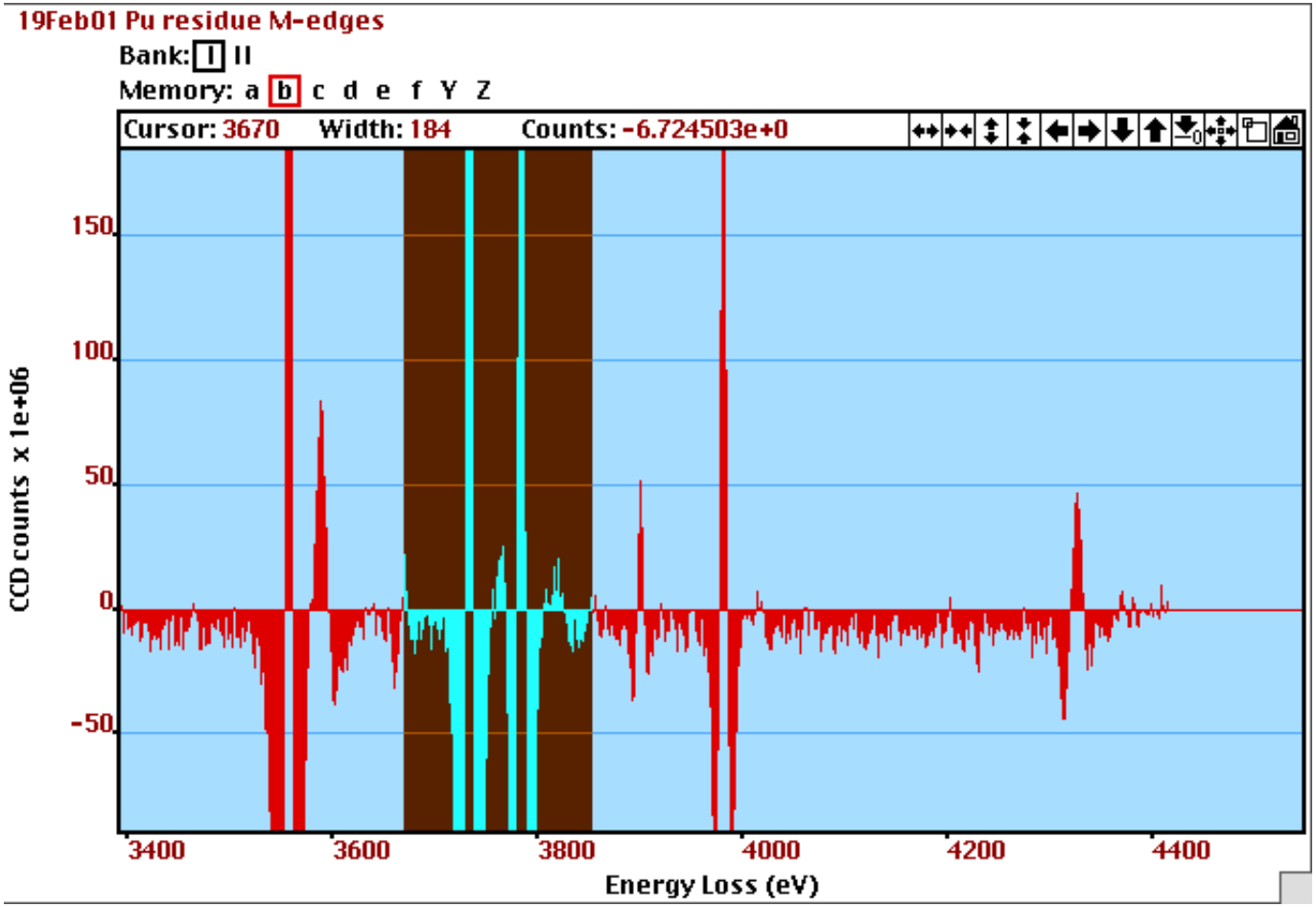

Figure 3.2. EELS of CSNF Material Showing Separation of 184 eV Between the Two Features Corresponding to the Np-M_5 and Np-M_4 Peaks

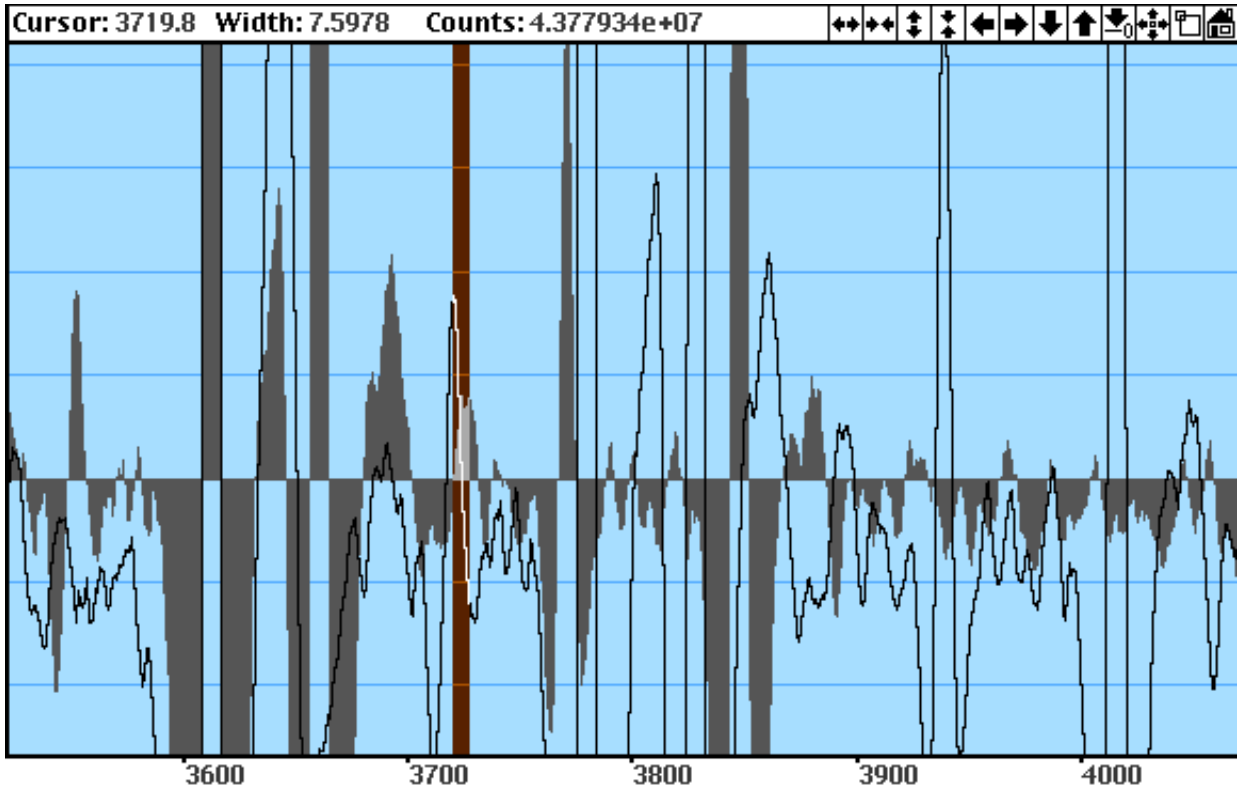

Figure 3.3. Two Identical Spectra, Except that One (the solid line) Has Been Shifted Exactly 176 eV. The U-M_4 edge of one spectrum has been superimposed on the U-M_5 of the other spectrum. A window has been drawn over the separation between two features in the spectrum. This window is 7.6 eV wide and corresponds to the Np-M_4 energy (3850 eV) minus the Np-M_5 energy (3665) – 176 (the shift energy). If both peaks were due entirely to plural scattering of the U, then they would overlay exactly. This is proof that Np is being detected in this spectrum.

In Figure 3.5a, the measured peak-to-peak separation is 178 eV for the U and 182 eV for the "Np" regions. This gives a calibrated energy of about 180 eV ±1 eV. In Figure 3.5b, the data were collected on a PEELS system. The total counts (20,000+) in the Np-M_5 region suggest that a visible peak should be present after the U-M_4 if plural scattering is the dominant process. However, the lack of a distinguishable peak in the Np-M_4 can be explained from chemical considerations. The intensity of the Np M_4 edge is much lower than for the earlier actinides in the series. This tends to support the assertion that Np can be detected and is in some uranyl phases.

The spectrum obtained from the uranium (VI) phase, weeksite [ideally $K_2(UO_2)_2(Si_2O_5)_3 \bullet 4H_2O$], was run through a peak fitting program to obtain more reliable estimates of the peak energies and the peak separation. These estimates are consistent with the values obtained with the EELS program and support the assertion that Np is incorporated into the weeksite phase (Buck and Fortner 1997). It is possible to calibrate spectra accurately by comparing them against the Np standard spectrum that is shown in Figure 2.1. The U-M edges from two alteration-phase spectra have been matched against the U-M edges on the Np standard sample (this phase contained Np, U, and trace Pu) (see Figure 3.6). The green-line of the Np standard spectrum lines perfectly with that from the blue spectrum (uranyl alteration phase) but not as well with the red. Again, if the peaks were entirely due to plural scattering, the match would not be made.

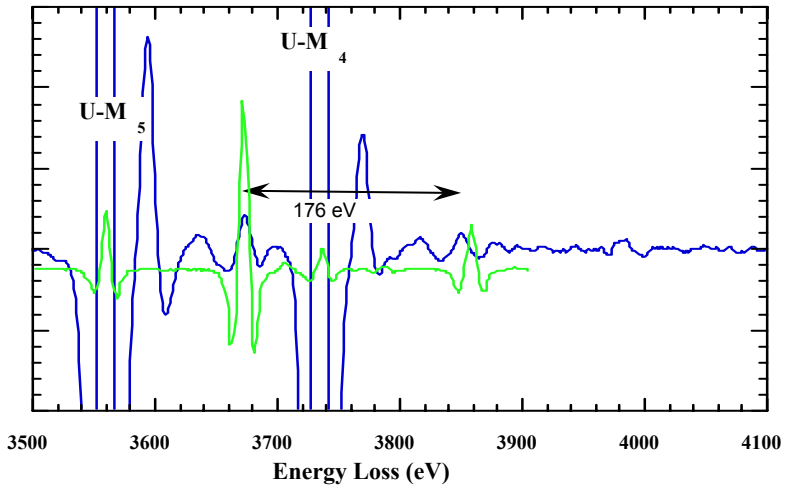

Figure 3.4. Comparison of Plural Scattering Peaks from a thick U-Only Sample and the Np Spectrum from Figure 2.1

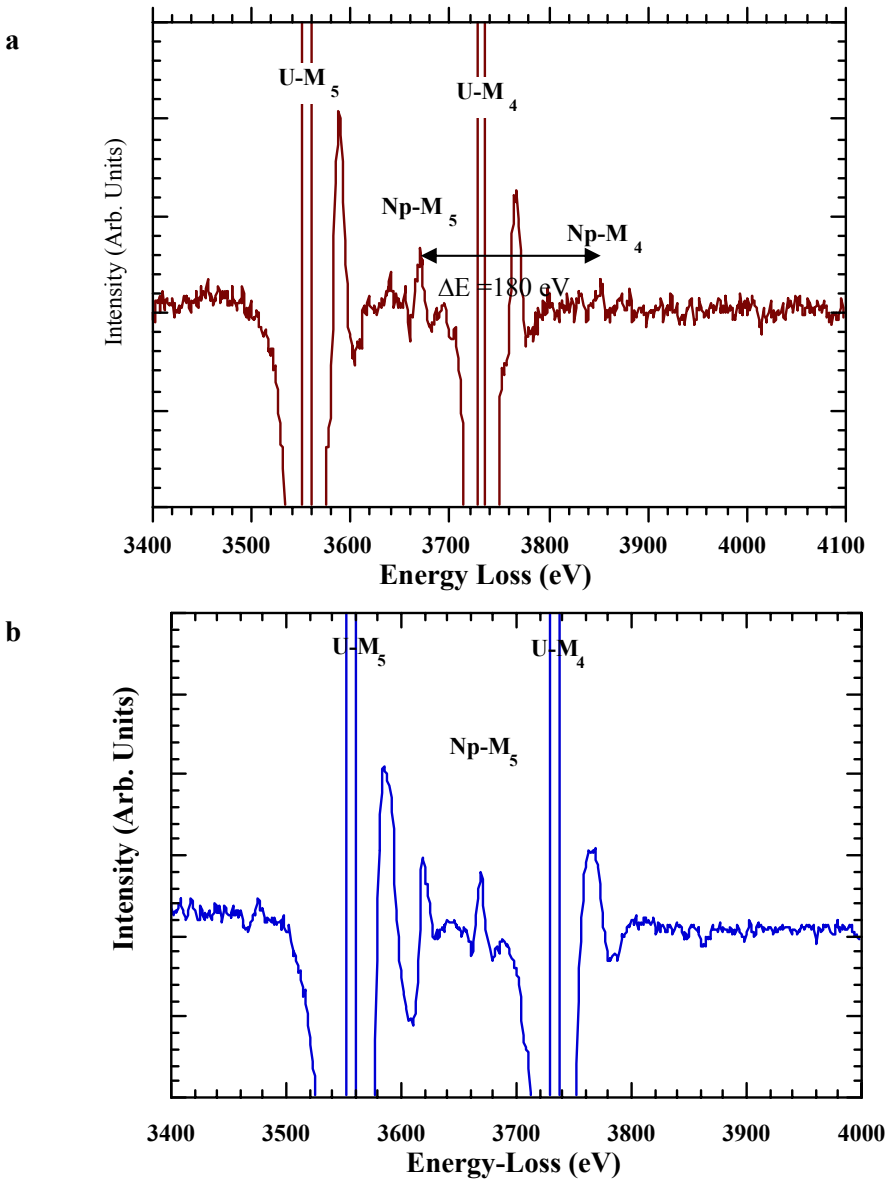

Figure 3.5. (a) Data Present in Buck et al. (1998) and (b) Obtained from Alteration Phases in a CSNF Sample

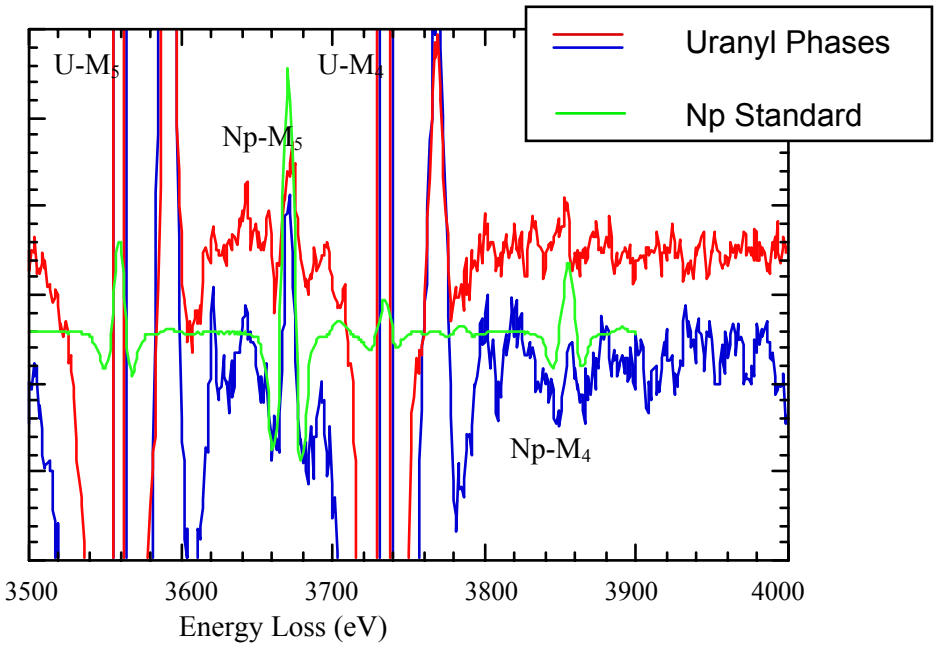

Figure 3.6. Electron Energy-Loss Spectra of a Uranyl Alteration Phase, Showing an Energy Separation that is Consistent with Np Being Associated with the Phases (red-line). Data obtained from a CSNF corrosion test (blue line). Obtained from an SRL131A glass test. The M4,5 edge energy separation on the Np standard (green line) was 184.4 eV.

4.0 Np Incorporation into U(VI) Studtite

The fundamental problem addressing the issue of Np behavior in weathered waste forms is the low level of Np in the starting material. The CSNFs tested have about 400 to 600 ppm Np. This is below the limit of detection of energy dispersive x-ray spectrometry (EDS) systems on TEMs and scanning electron microscopy (SEMs) because of low signal-to-noise and overlap problems with the many other elements in spent fuels. Although radiochemical methods, inductively coupled plasma-mass spectrometry (ICP-MS) methods, and X-ray absorption spectroscopy (XAS) with a Synchrotron source do have the capability of detecting such levels of Np in spent fuel, the low spatial resolution of these methods together with relatively imprecise sampling means that we will not be able to determine the disposition of Np in any alteration phase with these techniques. To date, the only method available is EELS on a TEM. However, this technique is extremely difficult because of the specific energy region that must be used. To date, only a few examples of possible Np incorporation into an alteration phase have been found. Although these data have been widely used to support the concept of Np incorporation, there has been little experimental evidence from spent-fuel tests on Np incorporation into uranyl alteration phases (e.g., β-uranophane and boltwoodite). However, even if unequivocal evidence for Np incorporation had been found in the Argonne tests, would this be valid for a repository model? As these tests were only carried out under one set of conditions, they may not be valid for all water chemistries.

4.1 Analysis of Laboratory-Synthesized Np-Doped Studtite

A Np-doped studtite was prepared and then examined the solid with X-ray diffraction (XRD) and TEM. The starting Np was held in the (V) oxidation state with $NaNO_2$. Ultra-violet spectroscopy was used to establish the oxidation state. Uranyl nitrate (0.5 g) was reacted with 1 M H_2O_2. The resultant product in the U-only test was a light yellow white solid, consistent with studtite. To produce the Np-bearing U solid, we added the Np(V) solution to the reacting uranyl nitrate solution.

The resulting solid that precipitated was red-brown (the pure U studtite was white). A green coloration remained in the solution, indicating the presence of some residual Np(V). Characterization of the U phase and Np-doped U phase was performed with optical microscopy, XRD, infrared (IR), and TEM.

In Figure 4.1a, an example of an EDS spectrum of the U solid is shown. It was not possible to quantify the amount of Np present, as standards were not available, but it appears to be around 10% of the U based on EDS simulations (see Figure 4.1b). The EDS results demonstrate how difficult it is to detect Np even at relatively high levels; however, with a complete set of standards, it should be possible to model the peak shapes, allowing lower detection limits. In contrast, EELS was easily able to detect this level of Np in the solid. The sample used was not ideal for EELS (see Figure 4.2).

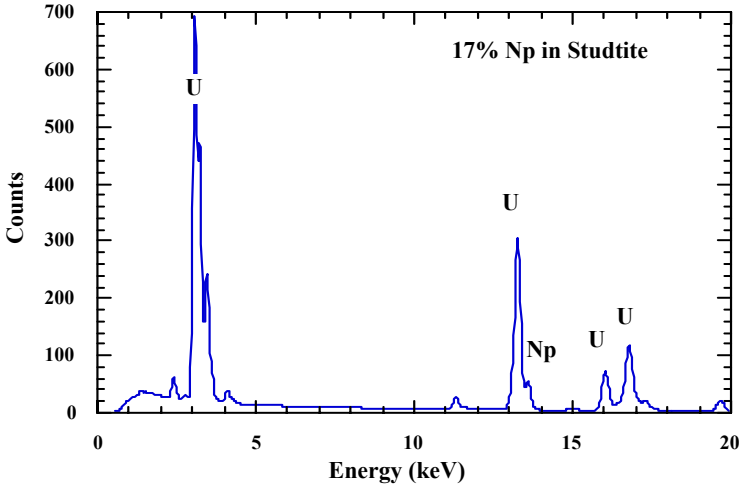

(a)

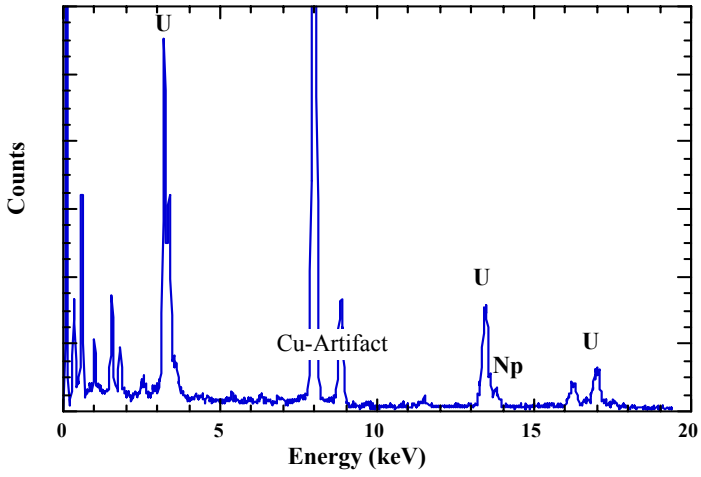

(b)

Figure 4.1. (a) Simulated Spectra of Np-Doped Studtite and (b) Experimental Analysis of Doped Solid

The EELS analysis is the best evidence for incorporating Np into this phase. The actinide N-edges were analyzed, and although they are very weak, they are at a lower energy and easier to obtain in radiation-sensitive materials. X-ray diffraction of the U phase and the Np-doped material were both consistent with studtite. No other minor phases were detected.

Further evidence for the purity of the U and Np-doped solids was obtained from IR spectroscopy (see Figure 4.3). Both IR spectra are similar and show several interesting features. The spectrum in the 3000 to 3500 cm^{-1} region is characteristic of bonded water and typical of the layered uranyl (VI) oxide phases.

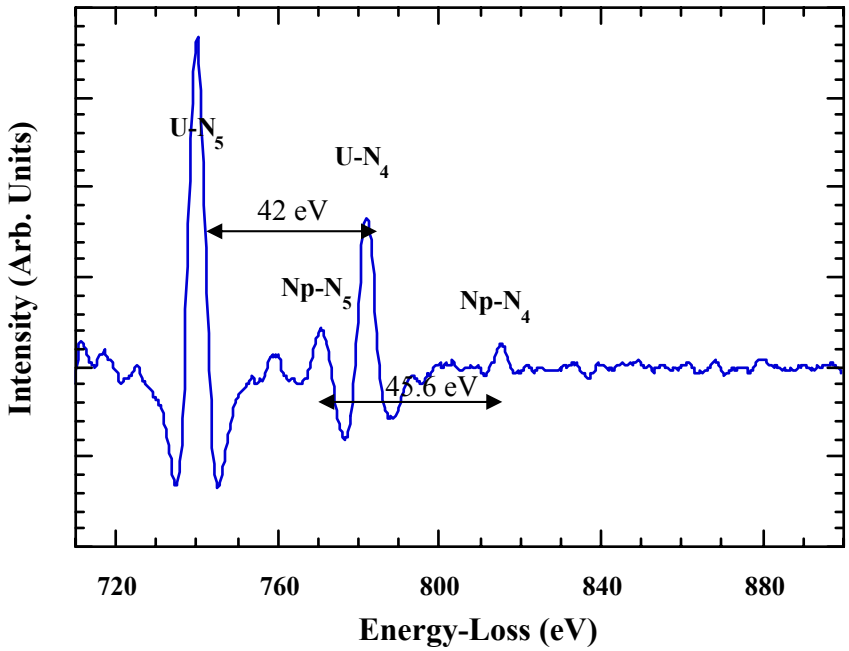

Figure 4.2. EELS evidence of Np in a Synthetic U phase (studtite)

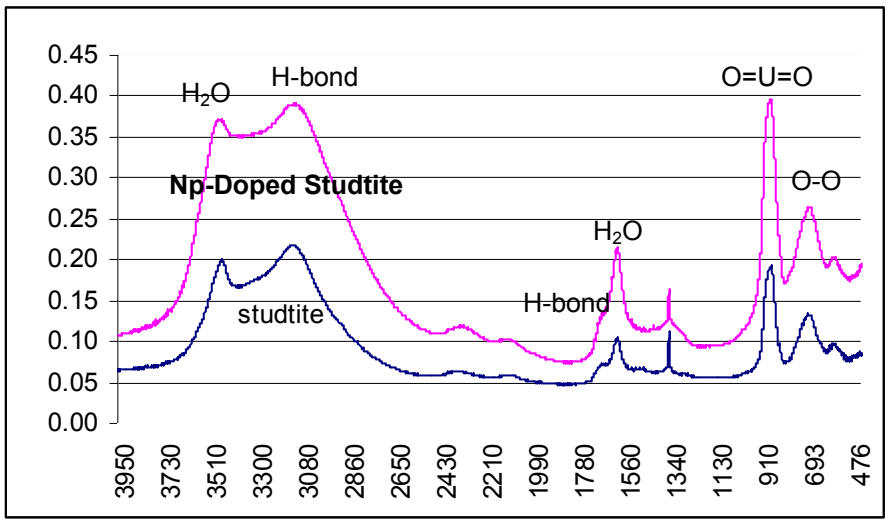

Figure 4.3. Infrared Spectrum of Studtite and Np-Studtite (KBr Pellet)

4.2 Analysis of Np Incorporation into Uranophane

A series of Np-bearing U(VI) phases were prepared at PNNL (Douglas et al. 2003). In the first set examined, a number of uranophane synthetic mineral phases were analyzed. Optical microscopy of the samples revealed clear differences between the U-only and Np-doped samples (see Figure 4.4). Each of the uranophane samples possessed a different color, and in the TEM, there was no obvious evidence of phase separation. The TEM at the EMSL DOE User Facility was used in this study.

The analysis demonstrated the presence of Np in the uranophane phases. In Figure 4.5, screen-shots from the Gatan EELS software program show that the distances between the Np-M_5 and Np-M_4 edges are clearly 184 eV. Because a smaller energy dispersion was chosen, the separation in the energy peaks was much more certain, as the peaks were separated by twice the number of channels. These examples prove the ability of EELS to detect Np in a U-only matrix.

Figure 4.6 shows two different concentrations of Np in uranophane. The U-spectra overlap perfectly. Two windows, both 176 eV wide, have been superimposed on the plot. The energy difference between the two edges labeled "Np" are clearly separated by more than 176 eV. Indeed, the separation is consistent with the Np-M_5 to Np-M_4 splitting. [If plural scattering dominated under these conditions, variation in the intensity of the Np-M_5 feature would not be expected.] The Np intensity in one case (the red spectra) is similar to that observed from some of the CSNF samples from the vapor hydration tests.

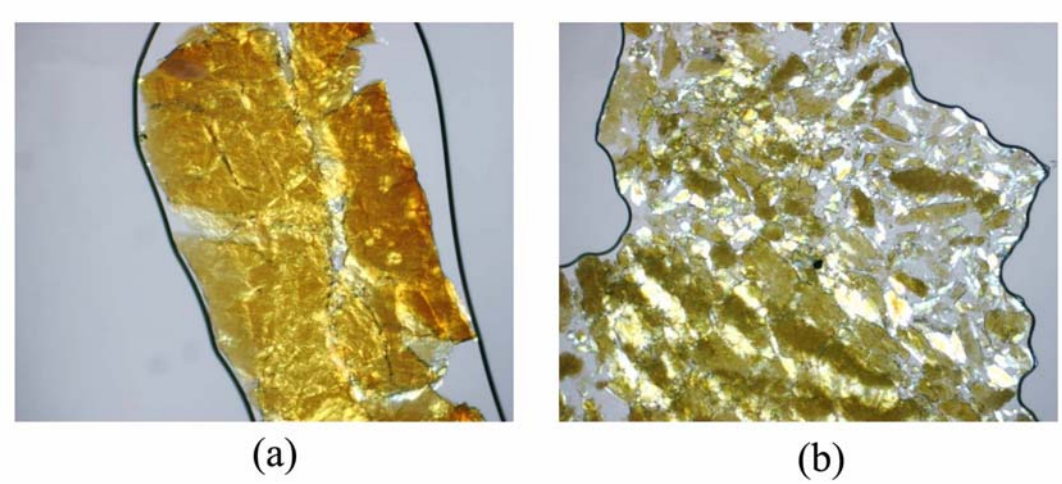

Figure 4.4. Optical Images of Uranophanes (a) Non-doped and (b) Np-Doped Uranophanes

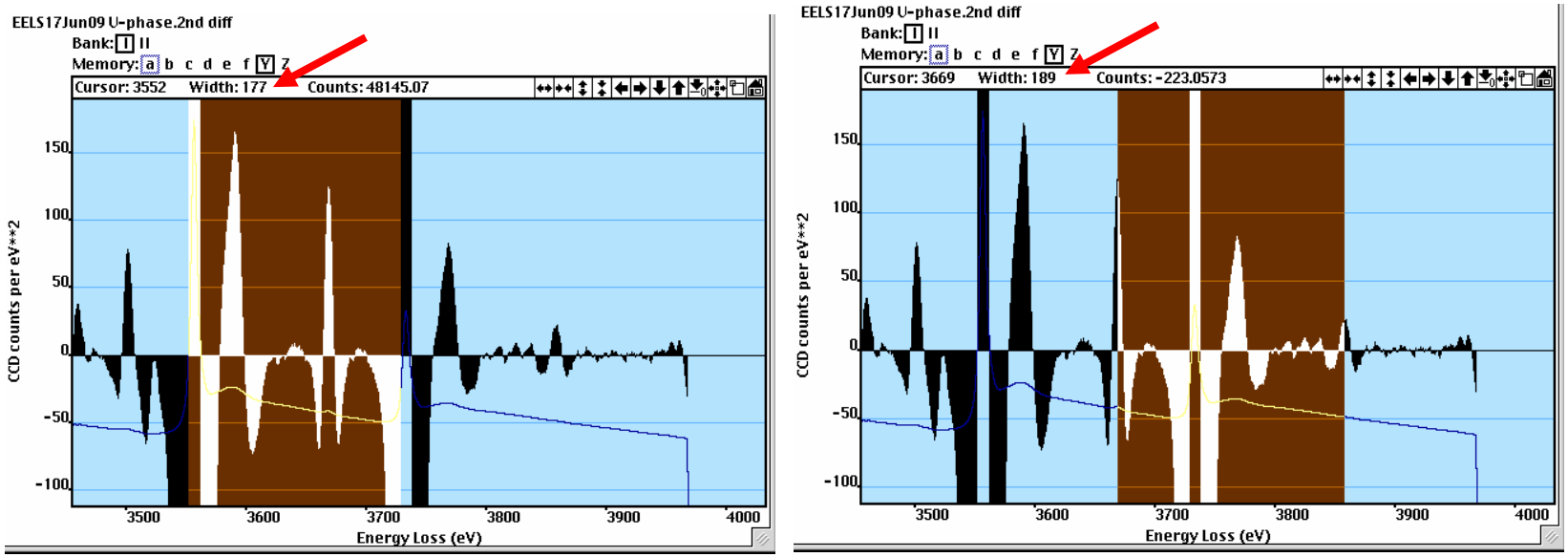

Figure 4.5. Screen Shots from the Gatan Program EL/P Showing the ~176-eV Window Between the U M-Edges and the ~189-eV Window Between the Np M-edges. The red arrows point to the energy-width value.

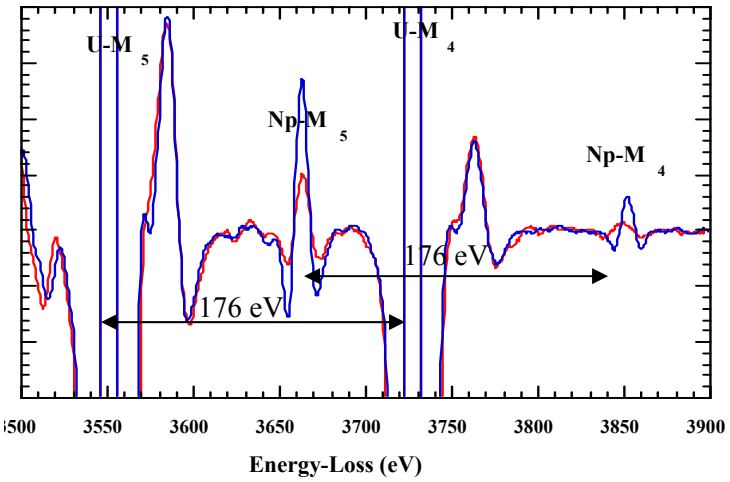

Figure 4.6. Electron Energy-Loss Spectrum of Uranophane Solid Containing Low and high Concentrations of Np.

4.3 Analysis of Spent Fuel Studtite Phases

In recent experiments at PNNL, the observed alteration products on spent fuel were different from those observed on UO_2 tests. In the spent-fuel tests, studtite was observed to be the major alteration phase. Meta-studtite $[UO_2(O_2)(H_2O)_2](H_2O)$ has been commonly found in the Hanford K-Basin sludges. Additionally, the material has been characterized in high concentration on the cladding of K-East Basin Fuel elements (Abrefah et al. 1998).

The formation of the uranyl (VI) peroxide mineral phase studtite and meta-studtite was observed as the exclusive alteration phases on corroding spent nuclear fuel (see Figure 4.7). These products were formed after immersion in deionized water over a two-year period. A fraction of the samples was additionally observed as an interfacial suspension. Radiochemical analysis of the dried suspensions indicated that ^{237}Np may be incorporated with the uranyl (VI) peroxide. The structures of the uranyl (VI) peroxy and neptunyl (VI) peroxy species may be similar enough to account for this behavior. Pu, Cm, and Am were found to be in lower concentration in the uranyl phases; however, 5 to 6% of the available Pu and Am, based on radionuclide inventory calculations provided by Guenther et al (1986), was co-precipitated with the uranyl phase.

The radiochemical analysis of the filtered liquids and interfacial films from the spent-fuel samples is presented in Table 4.1. The U fraction in the filtered liquid samples was determined by Kinetic Phosphorescence Analysis (KPA). The interfacial films were digested, and the total U was also determined by KPA in triplicate for sample 25-P_7. In Table 4.2 data are reproduced from hydration tests performed on the same spent fuel in leaching studies performed between 1985 and 1990 at PNNL. For consistency, the radiochemical data are presented in Table 4.2 as µg-analyte per g-U for comparison to the inventory calculations for 30.2 MW/d burn-up fuel at 16 years (Guenther et al. 1986).

The liquids data indicate similar magnitudes of radionuclides at 25°C. In the 60°C sample, the fraction drops off as more U was dissolved in the five-week period the sample was at temperature. The samples 25-P_2, 25-P_7, and 60-P_5 each had different amounts of liquid due to evaporation, but also the solution pH

was lower at 60ºC. This observation at 60ºC also occurred for hydration studies on sintered unirradiated fuel over a two-year period and may be due to the solubility of absorbed CO_2.

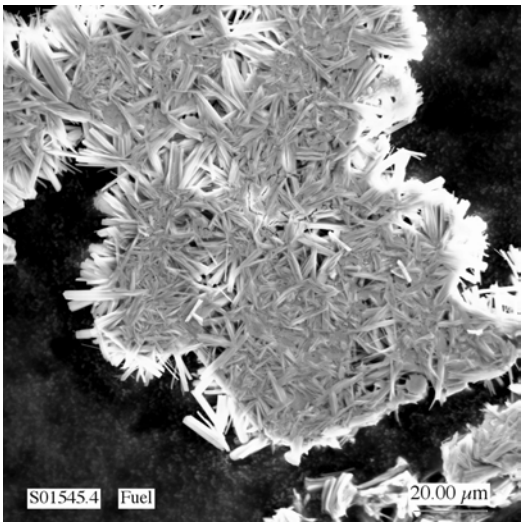

(a)

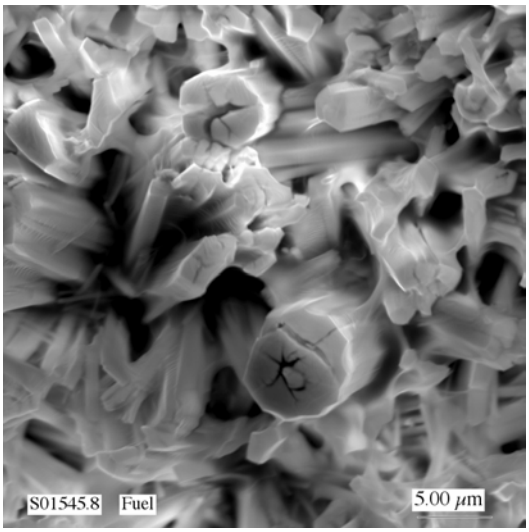

(b)

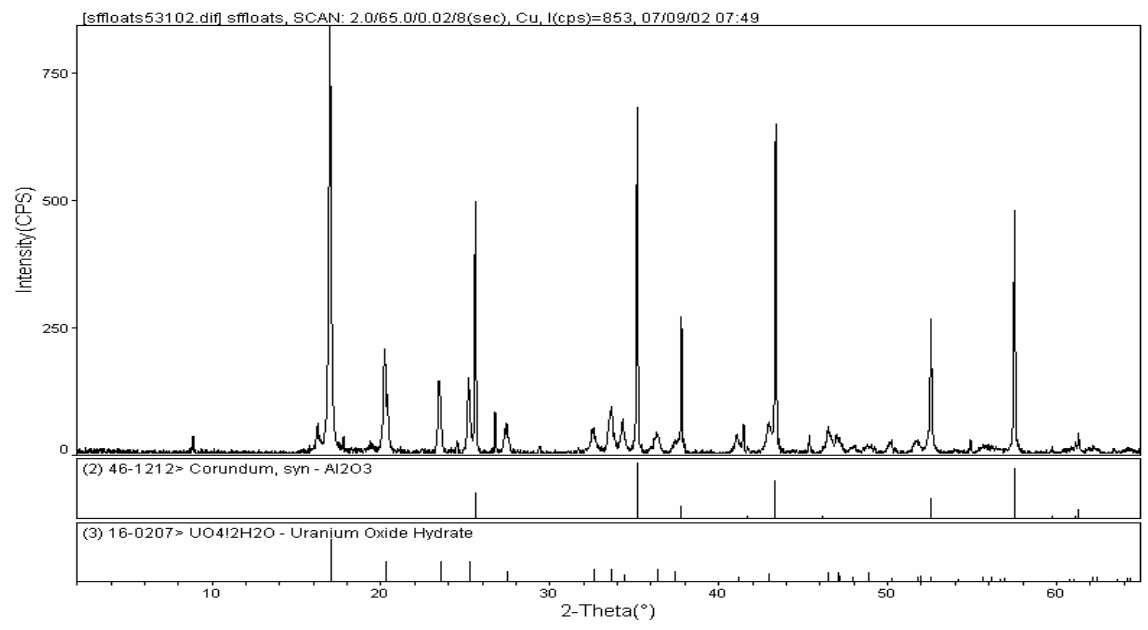

(c)

Figure 4.7. (a) Low Magnification SEM Picture of Meta-Studtite Released from the Surface of Corroded Spent Nuclear Fuel and (b) Higher Magnification Image Showing an Individual Crystallite. The drying in the microscope vacuum chamber may have resulted in the cracking in the particles. (c) X-ray diffraction scan of studtite.

Table 4.1. Radiochemical Analysis of Dried Films from SNF after 1.5 Years of Immersion

Sample	Total U (µg)	^{237}Np µg/g U	^{239}Pu µg/g U	^{241}Am µg/g U	$^{243+244}$Cm µg/g U
25 P_7	623	330	943	32.3	0.62
Radionuclide Inventory (Guenther et al. 1986)		345	12200	516	15.8
Percentage Uptake		96%	8%	NV	4%
NV= Not valid – fuel age not taken into account in radionuclide inventory values.					

Table 4.2. Radiochemical Analysis of Leachates from SNF after 1.5 Years of Immersion

Sample	pH	Total U (µg/mL)	^{237}Np µCi/mL	^{239}Pu µCi/mL	^{141}Am µCi/mL
25 P_2	6.2	6.9E-01	6.1E-05	1.7E-04	4.2E-03
25 P_7	6.3	1.5E+00	6.9E-05	2.7E-04	9.3E-03
Wilson	8.4	0.2	2.0E-07	3.0E-05	1.0E-04

5.0 Discussion

This study demonstrates that EELS is capable of detecting low levels of Np in a uranium matrix provided an energy dispersion is used that allows sufficient channels between features. There is clear evidence for Np incorporation into U(VI) phases from laboratory-synthesis experiments; however, further work needs to be done on the CSNF experiments under various conditions to justify the case for Np co-precipitation with uranium (VI) phases. Burns [(a)] has pointed out the importance of counter ions such as Na to substitute into the interlayer to provide for a charge-balance mechanism. Uranium-bearing phases reported from the spent fuel vapor drip tests tended to contain Ca and Cs (Buck et al. 1998) which may account for these phases containing Np. In spent fuel, stable Cs could also act as a charge compensating ion, as well as any ions from other waste-package materials, including Na^+ and K^+. Experiments looking at Np incorporation by Finch et al (2002) did not include counter ions which may account for the lack of Np incorporation observed.

New advancements in EELS instrumentation should provide improved detection capabilities. For instance, the Gatan TRIDIEM, has more energy channels (2048 Ch) and greater dynamic range (0-60 000 counts) than the GIF2000 (1024 Ch and 0-16 000 counts/Ch) instruments. This would allow one to observe the U and Np M-edges at an energy dispersion of 0.3 eV. Although the $N_{4,5}$ edges are very weak, they can be used for analysis in solids that do not contain other elements and will be devoid of interferences, as long as the EELS energy resolution <1.5 eV. The N-edges could not be used during the analyses of spent fuel corrosion products, as other trace elements, including barium, interfered with the analysis.

5.1 Effect of Oxidation Potential on Np behavior

Burns et al. (2002) have demonstrated incorporation of Np(V) into uranophane and Na compreignacite structures in concentrations equivalent to what was present in solution. Furthermore, Burns [(a)] suggest that counter-ions will increase the Np incorporation into these phases as well. Experiments reported in this study clearly indicate the formation of studtite-related phases with significant uptake of Np. The studtite was present in these fuel tests after two years. Studtite also appears to be a stable phase in these tests. The oxidation state of the Np in studtite may be (VI) which may make Np incorporation easier; however, the studtite structure consists of chains of uranyl ions rather than the layered motifs typical of schoepite and uranophane phases. This chain-type structure may be more accommodating of the slight structural differences between uranyl and neptunyl groups.

5.2 Retention of Np during Borosilicate Glass Dissolution

Although the total amount of Np in borosilicate glass is low, glass tests are useful because the total amount of reaction can be quantified by measuring boron release. Instead of reporting Np concentrations, actinide studies on glasses have tended to report a retention factor. This is a more useful value when the total amount of the released element in question does not approach a solubility limit. Retention factors are useful for observing co-precipitation behavior. The ratio of Np to U in borosilicate-glass formulations is similar to the ratio in the spent fuel. During glass reaction, released U will precipitate as weeksite or sometimes uranophane. Several groups have analyzed Np-doped glasses.

(a) Manuscript in preparation (2003).

Data from high level waste borosilicate glass tests have tended to show congruent release of Np and U with boron (Ebert 1995; Bates and Buck, 1994). It is generally assumed that Np in borosilicate glass is present in the (V) oxidation state; hence, no oxidation step is required for removal of Np from the surface. As the reaction proceeds, U concentrations can result in precipitation of U as weeksite. In the glass drip tests that show similar release of Np, secondary U phases have not been observed.

In Figure 5.1, data extracted from Ebert (1995) demonstrates the co-behavior of Np and U. This result does not support Np incorporation.

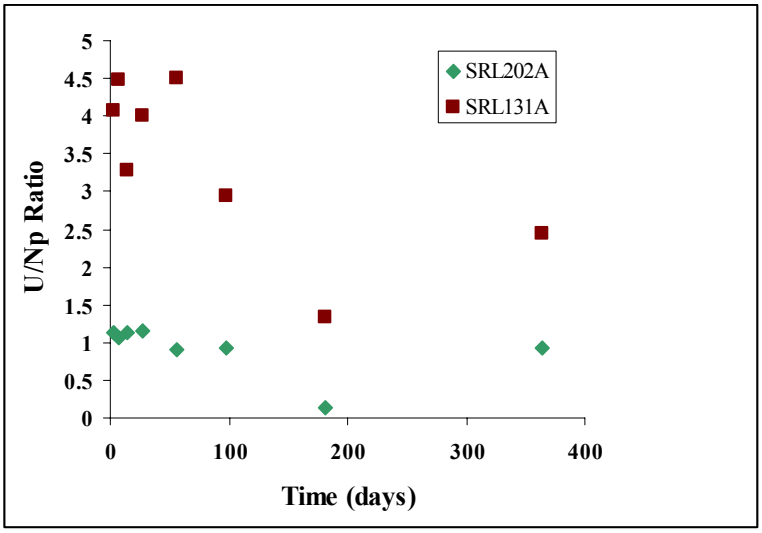

Figure 5.1. Normalized Mass Losses of U/Np for SRL131A and SRL202A Glasses Reacted at 20,000 m^{-1} (extracted from Ebert [1995])

6.0 Conclusions

By looking at the energy gap between the Np M-edge "white-lines," an estimate of Np incorporation may be obtained. However, the energy difference is small, on the order of 7 to 8 eV. Poor energy resolution in the spectrum may easily mask the effect. By using smaller energy dispersions (e.g., ≤0.5 eV/Ch), the plural peak and the Np peak will be separated by more channels and can be more easily identified. The analysis of Np-doped uranophane samples demonstrates the advantage of using a lower energy dispersion. The plural peaks that occur in U samples have been observed in many spectra, in some cases preventing confirmation of the presence of Np; however, analyses of corrosion products using the energy-separation method has provided evidence of Np in some cases.

The results of the laboratory experiments with studtite and Np-doped studtite indicate that this phase can incorporate a significant amount of Np. This result was confirmed with XRD, IR, and TEM-EELS. The results from the preliminary studies with spent fuel also suggest significant uptake of Np. However, these results need to be duplicated over a larger range of relevant conditions. Synthesized uranophanes show clear evidence for the incorporation of Np.

The evidence of Np incorporation into uranyl (VI) phases is not well established in CSNF tests, but there is strong evidence for similar chemical behavior for U and Np in a number of experiments. The difficulties of testing spent fuel and detecting Np will continue to cause problems in this area, and it is unlikely that continued testing with spent fuel will resolve this issue. In the light of new studies by Burns et al.[(a)] and Douglas et al. (2003) that demonstrate ready uptake of Np into uranophane, the role of secondary U (VI) phases in attenuating Np, either through sorption or incorporation, may be significant in a repository environment.

Electron energy-loss spectroscopy can be a suitable technique for determining the presence of low levels of Np in U-bearing solids in spite of artifact problems. No other technique has sufficient spatial resolution combined with sensitivity. Improvements in instrumentation, such as the Gatan TRIDIEM will further improve the ability to detect these low level transuranics.

6.1 Recommendations

- Examination of CSNF and related samples should be attempted with a low energy dispersion on the EELS instrument. This report has demonstrated that the detection of Np with the M-edges can be accomplished at 0.5eV/Ch energy dispersion; however, on instruments with more energy channels, such as the Gatan TRIDIEM, even lower energy dispersions would further improve low level detection.

- EELS analysis with the $N_{4,5}$ edges is probably only effective with Np-only doped solids, although this region is not subject to the type of plural scattering experienced by the M-edges. This is because these are edges are very weak and there can be overlap with other elements.

- New corrosion tests on Np-doped solids should be repeated with charge-compensating ions included. Tests should be conducted over a range of pH and Eh. The effects of thin-film radiolysis on Np incorporation should also be quantified.

(a) Manuscript in preparation (2003).

7.0 References

Abrefah J, SC Marschman, and ED Jensen. 1998. *Examination of the Surface Coatings Removed from K-East Fuel Elements*. PNNL-11806, Pacific Northwest National Laboratory, Richland, WA.

Bates JK, and EC Buck. 1994. "Results of drip tests on sludge-based and actinide-doped glasses." In: *International High Level Radioactive Waste Management Conference,* Las Vegas, NV, May 22-26.

Buck EC. 1999. "Second difference electron energy-loss spectroscopy with the Gatan Image Filter." *Microsc. Microanal.* 5:808-809.

Buck EC, RJ Finch, PA Finn, and JK Bates. 1998. "Retention of neptunium in uranyl alteration phases formed during spent fuel corrosion." *Mater. Res. Soc. Symp. Proc.* 506:87-94.

Buck EC, DJ Wronkiewicz, PA Finn, and JK Bates. 1997. "A new uranyl oxide hydrate phase derived from spent fuel alteration." *J. Nucl. Mater*. 249:70-76.

Buck EC, and JA Fortner. 1997. "Detecting low levels of transuranics with electron energy loss spectroscopy." *Ultramicroscopy* 67:69-75.

Burns PC, ML Miller, and RC Ewing. 1997. "Incorporation mechanisms of actinide elements into the structures of U^{6+} phases formed during the oxidation of spent nuclear fuel." *J. Nucl. Mater*. 245**:**1-9.

Burns PC, and KA Hughes 2002. "Studtite, $[(UO_2)(O_2)(H_2O)_2](H_2O)_2$: The first structure of a peroxide mineral." *Amer. Miner*. 88:1165-1169.

Ebert WL. 1995. *The Effects of the Glass Surface Area/Solution Volume Ratio on Glass Corrosion: A Critical Review.* ANL-94/34, Argonne National Laboratory, Argonne, IL.

Douglas, M, SB Clark, S Utsunomiya, RC Ewing, EC Buck, and BD Hanson. 2003. "Neptunium association with uranium (VI) silicate solid phases." In: *Migration'03,* Gyeongju (Kyongju), Korea, September 21-26, 2003.

Finch RJ, and RC Ewing. 1992. "The corrosion of uraninite under oxidizing conditions." *J. Nucl. Mater.* 190: 133-156.

Finch RJ, JA Fortner, EC Buck, SF Wolf. 2002. "Neptunium incorporation into uranium (VI) compounds formed during aqueous corrosion of neptunium-bearing uranium oxides." *Mater. Res. Soc. Symp. Proc.* 713: 647-654.

Finn PA, EC Buck, M Gong, JC Hoh, JW Emery, LD Hafenrichter, JK Bates. 1994. "Colloidal products and actinide species in leachate from spent nuclear fuel." *Radiochem. Acta.* 66/67:189-187.

Guenther RJ, DE Blahnik, TK Campbell, UP Jenquin, JE Mendel, LE Thomas, and CK Thornhill. 1986. *Characterization of Spent Fuel Approved Testing Material ATM-103*. PNL-5109-103, Pacific Northwest National Laboratory, Richland, WA.

Distribution

No. of Copies

OFFSITE

4 Bechtel SAIC Company, LLC
1180 Town Center Drive
Las Vegas, NV 89144
Attn: Yueting Chen (2)
FJ Pearson
Howard Atkins
Christine Stockman

1 Argonne National Laboratory
9700 South Cass Avenue
Argonne, IL 60439
Attn: Dr. James C Cunnane (2)

1 Sandia National Laboratory
1515 Eubank SE
Albuquerque, NM 87123
Attn: Dr. Patrick V Brady

2 Australian Nuclear Science and Technology Organisation
New Illawarra Road, Lucas Heights, NSW 2234
Attn: Michael Colella
Dr. Katherine L Smith

No. of Copies

ONSITE

37 Pacific Northwest National Laboratory

Edgar C Buck (6)	P7-27
Brady D Hanson (20)	P7-27
Bruce K McNamara	P7-25
Judah I Friese	P7-22
Chong-Min Wang	K8-93
Jonathan P Icenhower	K6-81
Alice Dohnalkova	P7-50
Larry E Thomas	P8-16
Kenneth M Krupka	K6-81
John M Zachara	P8-96
Andrew R Felmy	P8-96
Technical Report Files (2)	P7-27